

can be ascribed to different Coulombic work terms associated with the higher charges, since the work-correlated rate constant (k_{cor}) and k_{obsd} are related by

$$\log k_{\text{cor}} = \log k_{\text{obsd}} + \frac{F}{2.303RT}(Z_r - \alpha_1)\phi_r \quad (9)$$

where ϕ_r is the potential at the reaction site with respect to the bulk solution, Z_r is the charge carried by the reactant, and α_1 is the intrinsic transfer coefficient.⁵¹ Differences observed in k_s for Hg, Au, and Pt are apparently due to a dependence on the ϕ_r term for the different electrodes, i.e. different double-layer effects result in different values of k_{obsd} . Similar electrode dependencies have been noted with complexes of Fe, Co, Mn, and Cr containing thia and oxa donor groups,⁵² and therefore, a specific interaction of the electrode with the cobalt amine cage complexes can be ruled out. However, the rate constants are complicated by adsorption of the complexes on the electrodes and a more detailed analysis of the applicability of the Marcus-Hush theories in terms of heterogeneous and homogeneous rate characteristics of the cage complexes is continuing and will be described at a later date.

- (51) Weaver, M. J. *J. Phys. Chem.* **1980**, *84*, 568-576 and references therein.
 (52) Bond, A. M.; Martin, R. L.; Masters, A. F. *Inorg. Chem.* **1975**, *14*, 1432-1435.

Conclusions

The use of the Co(III/II) reduction potentials of substituted cage complexes is a new and effective method for obtaining substituent effects. It is not limited to studying the substituents listed in this paper, and work is proceeding toward expanding the series. In addition, work is in progress for obtaining detailed solvent dependencies and temperature dependencies of polar substituent constants. These are important areas to investigate, since a single source for such constants is still not available.³¹ The comparatively large NMR coupling constants between the apical carbons and the metal ions can also be analyzed in terms of a mechanism similar to that given here.⁵³

Acknowledgment. We wish to thank the ANU NMR Service for the many ¹³C NMR and ⁵⁹Co NMR spectra, Dr. J. Bromilow for many helpful and stimulating discussions, and Drs. J. MacB. Harrowfield, R. J. Geue, and W. Petri for supplying some spectral results prior to publication.

Supplementary Material Available: Listings of observed and calculated redox potentials, ¹³C and ¹H NMR chemical shifts, and electronic absorption maxima of the Co(III) complexes (Tables SI and SII) and a plot of δ_{Co} vs $E_{1/2}$ (Figure S1) (9 pages). Ordering information is given on any current masthead page.

- (53) Lay, P. A.; Sargeson, A. M. *Inorg. Chem.* **1986**, *25*, 4801-4802.

Contribution from Department of Chemistry, Faculty of Science and Technology, Sophia University, Kioicho, Chiyoda-ku, Tokyo, 102 Japan, and Department of Electronic Chemistry, Graduate School at Nagatsuta, Tokyo Institute of Technology, Midori-ku, Yokohama, 227 Japan

Mechanism of Intramolecular Rearrangements of (Acetylacetonato)bis(4,4,4-trifluoro-1-phenyl-1,3-butanedionato)ruthenium(III)

Yoshimasa Hoshino,^{1a,2a} Ryouta Takahashi,^{1a} Kunio Shimizu,^{1a} Gen P. Satô,^{*1a} and Koichi Aoki^{1b,2b}

Received December 7, 1989

Time variations of mole fractions of the three isomers of $[\text{Ru}(\text{acac})(\text{tfpb})_2]$ ($\text{acac}^- = \text{acetylacetonate ion}$, $\text{tfpb}^- = 4,4,4\text{-trifluoro-1-phenyl-1,3-butanedionato ion}$) were measured in *N,N*-dimethylformamide at 90, 110, and 130 °C. They were analyzed by a numerical method for the reversible, first-order, triangular network reactions previously developed. The results show that the direct conversion between the *fc,de*-(tfpb)₂ isomer and the *cf,ed*-(tfpb)₂ isomer was forbidden, which indicates that the bond-rupture mechanism through trigonal-bipyramidal intermediates with a single rearrangement is more plausible than the twist mechanism. Analysis of the rate constants according to the former mechanism suggests that the rate of rupture of a particular Ru-O bond is mainly, but not completely, determined by the kind of the nearest β -substituents.

Introduction

A tris(β -diketonato)metal complex with three unsymmetrical β -diketonate ligands can have two geometrical isomers: the facial and the meridional forms. A number of studies have been directed to the stereochemical rearrangement of the geometrical and optical isomers of "slow" type³ tris complexes of various metals, for example, cobalt(III),⁴⁻⁷ rhodium(III),⁵ chromium(III),⁸ and ruthenium(III).^{9,10} Two basic pathways are generally considered

in explaining the kinetics of these reactions: twist mechanisms and bond-rupture mechanisms.¹¹ The former involves no bond breakage, and the latter involves five-coordinated intermediates, whose structures may be essentially square-pyramidal (SP) or trigonal-bipyramidal (TBP), each with a dangling ligand at the axial or equatorial position. The kinetics of these complexes have been interpreted by a combination of several bond-rupture mechanisms rather than a single mechanism. For instance, Girgis and Fay⁶ studied the interconversion of the four isomers of tris-(1-phenyl-1,3-butanedionato)cobalt(III) in detail and explained the kinetics in terms of a combination of paths through the TBP-axial and SP intermediates. It is difficult to obtain sufficient kinetic information for clarifying the mechanisms of intramolecular rearrangements when homoleptic tris complexes are employed.

When two of the three β -diketonate ligands are unsymmetrical ligands, A-B, and the third ligand, C-C, is symmetrical (general formula $[\text{M}(\text{A-B})_2(\text{C-C})]$), there can be three geometrical isomers, each having a pair of enantiomers. This type of complex is more suitable than tris complexes for inferring the isomerization mechanism, since a certain interconversion among the three

- (1) (a) Sophia University. (b) Tokyo Institute of Technology.
 (2) Present addresses: (a) Nihon University College of Pharmacy, 7-7-1, Narashinodai, Funabashi-shi 274, Japan. (b) Department of Applied Physics, Faculty of Engineering, Fukui University, 3-9-1, Bunkyo, Fukui-shi 910 Japan.
 (3) Hutchison, J. R.; Gordon, J. G., II; Holm, R. H. *Inorg. Chem.* **1971**, *10*, 1004.
 (4) Gordon, J. G., II; Holm, R. H. *J. Am. Chem. Soc.* **1970**, *92*, 5319.
 (5) Fay, R. C.; Piper, T. S. *Inorg. Chem.* **1964**, *3*, 348.
 (6) Girgis, A. Y.; Fay, R. C. *J. Am. Chem. Soc.* **1970**, *92*, 7061.
 (7) Fay, R. C.; Piper, T. S. *J. Am. Chem. Soc.* **1963**, *85*, 500.
 (8) Fontaine, R.; Pommier, C.; Guiochon, G. *Bull. Chim. Soc. Fr.* **1972**, 1685.
 (9) Gordon, J. G., II; O'Connor, M. J.; Holm, R. H. *Inorg. Chim. Acta* **1971**, *5*, 381.
 (10) Everett, G. W., Jr.; Horn, R. R. *J. Am. Chem. Soc.* **1974**, *96*, 2087.

- (11) Muettterties, E. L. *J. Am. Chem. Soc.* **1968**, *90*, 5097.

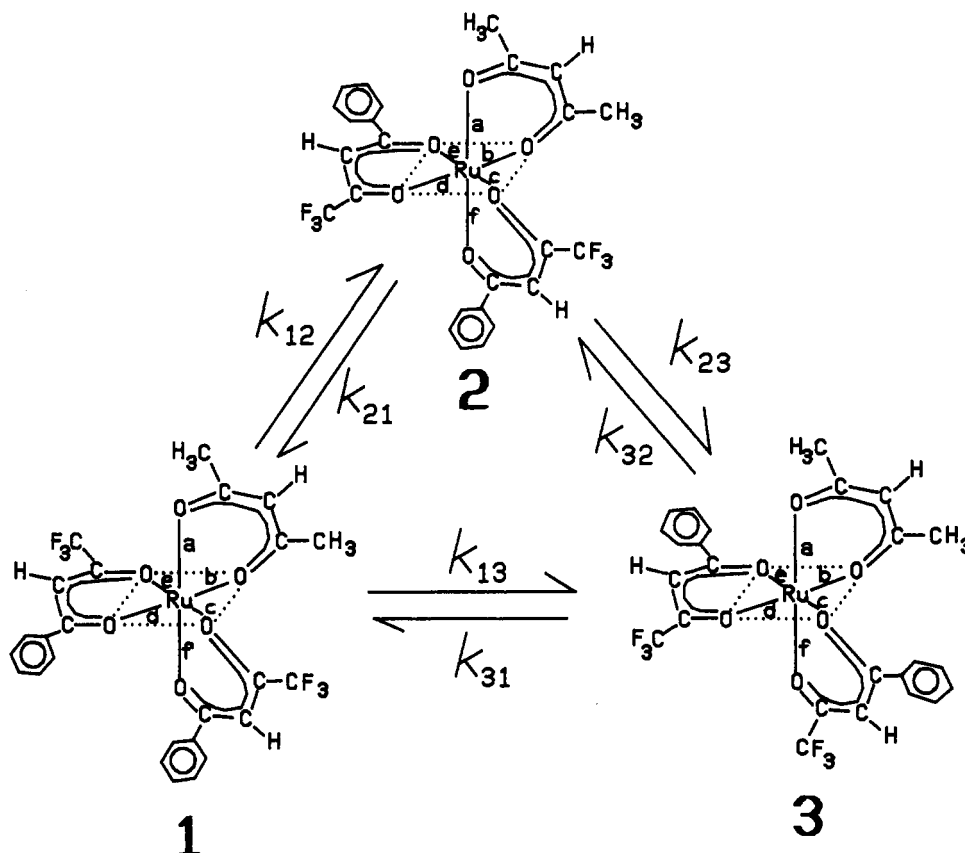


Figure 1. Triangular reaction mechanism.

geometrical isomers is impossible if the rearrangement occurs through the TBP transition states.¹² Nevertheless, study of the isomerization of $[M(A-B)_2(C-C)]$ complexes has been limited. Piper et al.¹³ determined the equilibrium constants of the isomerization reactions of (acetylacetonato)bis(1,1,1-trifluoro-2,4-pentanedionato)cobalt(III) at various temperatures by means of ¹⁹F NMR spectroscopy; but no kinetic study was carried out, because the isolation of the three geometrical isomers was unsuccessful.

In a previous paper,¹⁴ we reported a method for computing rate constants of reversible triangular network reactions by means of a nonlinear least-squares method. We described, as an example to show its applicability, a kinetic study of the intramolecular rearrangements between the geometrical isomers of a complex of the $[M(A-B)_2(C-C)]$ type, (acetylacetonato)bis(4,4,4-trifluoro-1-phenyl-1,3-butanedionato)ruthenium(III) in *N,N*-dimethylformamide (DMF) at 90 °C. We briefly mentioned the reaction mechanism.

The present paper deals with the same reaction. But more extensive results at different temperatures are presented, and the reaction mechanism is discussed in detail. The intramolecular rearrangement was successfully explained by a mechanism through TBP intermediates with single rearrangement.

Experimental Section

The three geometrical isomers are shown in Figure 1: *ab*-(acetylacetonato)-*fc,de*-bis(4,4,4-trifluoro-1-phenyl-1,3-butanedionato)ruthenium(III) (1), *ab*-(acetylacetonato)-*fc,ed*-bis(4,4,4-trifluoro-1-phenyl-1,3-butanedionato)ruthenium(III) (2), and *ab*-(acetylacetonato)-*cf,ed*-bis(4,4,4-trifluoro-1-phenyl-1,3-butanedionato)ruthenium(III) (3) (the designation follows the 1970 IUPAC rules¹⁵).

Table I. Equilibrium Constants in DMF^{a,b}

T/K (no. of runs)		K_{12}	K_{23}	K_{31}
363 (9)	ln K	0.593 ± 0.07	-0.394 ± 0.10	-0.200 ± 0.07
	K	1.81	$\begin{cases} +0.13 \\ -0.12 \end{cases}$	$\begin{cases} +0.07 \\ -0.06 \end{cases}$
383 (10)	ln K	0.579 ± 0.05	-0.394 ± 0.08	-0.185 ± 0.05
	K	1.78	$\begin{cases} +0.10 \\ -0.09 \end{cases}$	$\begin{cases} +0.06 \\ -0.05 \end{cases}$
403 (10)	ln K	0.565 ± 0.06	-0.406 ± 0.05	-0.158 ± 0.06
	K	1.76	$\begin{cases} +0.11 \\ -0.10 \end{cases}$	$\begin{cases} +0.06 \\ -0.05 \end{cases}$
	K	1.78 ± 0.10	$0.672 \begin{cases} +0.05 \\ -0.04 \end{cases}$	0.835 ± 0.05

^aThe uncertainties are 90% confidence levels. ^b $K_{ij} = x_{j,e}/x_{i,e}$, where $x_{i,e}$ and $x_{j,e}$ are the equilibrium mole fractions of isomer *i* and isomer *j*, respectively.

Their preparation and isolation have been described elsewhere.¹⁶ The reaction rates were measured by determining the mole fraction of each isomer in quenched reaction mixtures. High-performance liquid chromatography (HPLC) was used for the determination. The experimental details were described previously.¹⁴ No side reaction was detected at 90 and 110 °C. But thin-layer chromatography revealed the presence of a small amount of unidentified product when the reaction at 130 °C was prolonged beyond 2 h, and the data obtained within 2 h were used.

The HPLC peak area (defined as the product of the peak height and the half-peak width) was proportional to the amount of each isomer. The isomeric mole fractions were determined by means of calibration curves drawn for standard series of mixtures prepared gravimetrically from the isolated samples of the isomers.

Results

The equilibrium constant of the reaction $1 \rightarrow 2$ is defined as $K_{12} = x_{2,e}/x_{1,e}$ ($x_{1,e}$ and $x_{2,e}$ are the mole fractions of the specified isomers at the equilibrium), and K_{23} and K_{31} are defined analo-

(12) Pignolet, L. H.; Lewis, R. A.; Holm, R. H. *J. Am. Chem. Soc.* **1971**, *93*, 360.

(13) Palmer, R. A.; Fay, R. C.; Piper, T. S. *Inorg. Chem.* **1964**, *3*, 875.

(14) Hoshino, Y.; Takahashi, R.; Shimizu, K.; Satô, G. P.; Aoki, K. *Bull. Chem. Soc. Jpn.* **1989**, *62*, 993.

(15) *IUPAC Nomenclature of Inorganic Chemistry*, 2nd ed.; Butterworths: London, 1971; pp 57–63.

(16) Hoshino, Y.; Yukawa, Y.; Endo, A.; Shimizu, K.; Satô, G. P. *Chem. Lett.* **1987**, 845. Hoshino, Y.; Yukawa, Y.; Maruyama, T.; Endo, A.; Shimizu, K.; Satô, G. P. *Inorg. Chim. Acta* **1990**, *174*, 41.

Table II. Rate Constants in DMF^{a,b}

<i>T</i> /K	$k_{12}/10^{-4} \text{ s}^{-1}$	$k_{21}/10^{-4} \text{ s}^{-1}$	$k_{23}/10^{-4} \text{ s}^{-1}$	$k_{32}/10^{-4} \text{ s}^{-1}$	$k_{31}/10^{-4} \text{ s}^{-1}$	$k_{13}/10^{-4} \text{ s}^{-1}$	k_{21}/k_{23}
363	1.22 ₉ (1.22 ₀)	0.67 ₉ (0.67 ₄)	0.47 ₆ (0.47 ₃)	0.70 ₆ (0.70 ₁)	(0.02 ₇)	(0.03 ₃)	1.4 ₃
383	5.9 ₉ (6.0 ₀)	3.3 ₆ (3.3 ₆)	2.1 ₁ (2.0 ₄)	3.1 ₃ (3.0 ₂)	(-0.03)	(-0.03)	1.5 ₉
403	21.3 ₀ (21.3 ₇)	12.1 ₁ (12.1 ₅)	9.5 ₆ (9.4 ₆)	14.3 ₅ (14.2 ₀)	(-0.07)	(-0.08)	1.2 ₇

^a k_{ij} is the first-order rate constant of the reaction isomer $i \rightarrow$ isomer j . ^b The k values are calculated on the basis of the two-step consecutive reaction model (interconversion between isomer 1 and isomer 3 is forbidden). The figures in parentheses are calculated on the basis of the triangular-network reaction scheme (see text).

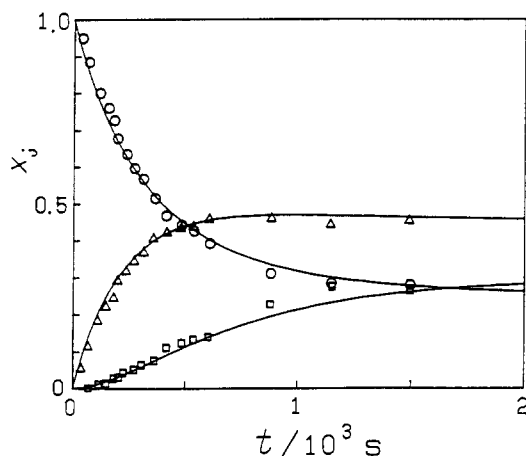


Figure 2. Variation of the mole fractions of 1 (O), 2 (Δ), and 3 (\square) with the time at 403 K when the starting species was 1. The curves are simulated from the nonlinear least-squares method.¹⁴

gously; only two of them are independent because $K_{12}K_{23}K_{31} = 1$.

The values of the equilibrium constants were calculated as follows. The HPLC peak areas (corrected for the relative sensitivities) of the isomers, A_j ($j = 1-3$), were measured with the reaction mixtures maintained at 90 and 110 °C for 2 days and at 130 °C for 2 h. The values of $\ln(A_2/A_1)$ and $\ln(A_3/A_2)$ were calculated for each run. Statistical tests indicated that they were independent of the starting species. After statistical treatment to reject outlying values, the mean values were taken to be $\ln K_{12}$ and $\ln K_{23}$, respectively. The results are given in Table I.

The variations of the mole fractions of the three isomers, x_j ($j = 1-3$), were measured at each temperature for the runs starting from each isomer. In this way, nine sets of the data, each consisting of the three x_j-t curves, were obtained. An exemplary set is presented in Figure 2. Shapes of these curves are similar to those in Figure 3A of ref 14.

The x_j-t curves were analyzed according to the numerical method previously described.¹⁴ For all the data, except those at 130 °C with starting species 1 and 2, the auxiliary kinetic parameters, p , q , r_i , and κ_i ($i = 1-3$),¹⁴ were evaluated successfully with standard deviations less than 10^{-4} . For the data at 130 °C with starting species 1 and 2, however, the original numerical method failed to converge even though a wide variety of initial values of the auxiliary parameters were tried, and the procedure had to be modified as follows. First, the r_i values were fixed and the values of p and q were adjusted by the least-squares method, and then the values of r_i were adjusted on holding the values of p and q constant. A set of nondiverging values of the parameters was obtained by repeating this procedure. It was still difficult to reduce the standard deviation to less than 0.01 owing to a very slow rate of convergence. The agreement of the best fit curves with the experimental data was satisfactory, as is seen from Figure 2; the standard deviation for these three curves (0.0117) was the worst of the nine sets of the data.

The values of k_{12} , k_{23} , and k_{31} were obtained from κ_1 , κ_2 , and κ_3 , which are linear combinations of the rate constants.¹⁴ The figures in parentheses in Table II are the k values thus calculated. These values of k_{31} and k_{13} are much smaller than the others at

Table III. Standard Enthalpies (ΔH^\ddagger) and Entropies (ΔS^\ddagger) of Activation in DMF, 363–403 K^a

reacn	$H^\ddagger/\text{kJ mol}^{-1}$	$\Delta S^\ddagger/R^b$
1 \rightarrow 2	84.0 \pm 18.8	-10.8 \pm 5.9
2 \rightarrow 1		-11.4 \pm 5.9
2 \rightarrow 3	88.3 \pm 19.5	-10.4 \pm 6.1
3 \rightarrow 2		-10.0 \pm 6.1

^a The uncertainties are 90% confidence limits. ^b R is the gas constant, ca. 8.314 J mol⁻¹ K⁻¹.

each temperature and almost the same as the experimental errors. The best fit values of k_{13} and k_{31} for 130 °C are even negative and, of course, meaningless. It is, therefore, reasonable to decide that the direct conversion between 1 and 3 is forbidden. Then the reaction mechanism reduces to a two-step consecutive reaction. The analytical expression in terms of the auxiliary parameters (eq 8 of ref 14) remains the same, but the contents of the auxiliary parameters are different. The same set of the numerical values of the auxiliary parameters were now solved for k_{12} , k_{21} , k_{23} , and k_{32} by putting $k_{31} = k_{13} = 0$. The results are given in Table II. The new set of values, naturally being in good agreement with the previous values obtained on the basis of the triangular scheme, is believed to be more precise.

Discussion

The K values (Table I) appear to depend slightly on the temperature, and the plots of $\ln K$ against T^{-1} were fairly straight lines. But their slopes were too small compared with the experimental errors to evaluate the standard reaction enthalpies, $\Delta_r H^\circ$, with any reliability (the largest in the magnitude was that for K_{31} , which amounted to only +1.3 kJ K⁻¹ mol⁻¹). Also in the case of the facial-meridional isomerization in DMF of several tris(trifluoromethyl-substituted β -diketonato)ruthenium(III) complexes, $\Delta_r H^\circ$ values were virtually zero.¹⁷ The $\Delta_r H^\circ$ of this type of isomerization will be appreciable only in a medium of low relative permittivity.¹⁷ Hence, we decide that the K values are independent of the temperature.

When the average values of K_{12} , K_{23} , and K_{31} are compared with the values expected if the equilibrium is determined only by the probability (2, 0.5, and 1, respectively), it is seen that isomers 1 and 3 are stabilized and isomer 2 is destabilized. But the standard Gibbs energies of the specific stabilization and destabilization are small, less than 1 kJ mol⁻¹. These energies will probably reflect the differences in the solvation entropies of the isomer molecules, since the standard reaction Gibbs energies of the isomerization are essentially entropic.

The standard enthalpies of activation, ΔH^\ddagger , and the standard entropies of activation, ΔS^\ddagger , were determined in the same manner as previously described (p 2556 of ref 17). They are listed in Table III. The ΔH^\ddagger values are similar to or smaller than the reported values for racemization or isomerization of tris(β -diketonato) complexes of metal ions other than ruthenium(III) in solution phases.^{4-6,8,9,17} The $\Delta S^\ddagger/R$ values correspond to preexponential factors of (2.7–9.3) $\times 10^6$ s⁻¹, which are significantly smaller than the values for those tris(β -diketonato)metal complexes (ca. 10^{12} – 10^{15} s⁻¹). Instead, the ΔS^\ddagger values are very close to those

(17) Kobayashi, K.; Satsu, Y.; Hoshino, Y.; Arai, S.; Hatakeyama, K.; Endo, A.; Shimizu, K.; Satô, G. *P. Bull. Chem. Soc. Jpn.* **1989**, *62*, 3252.

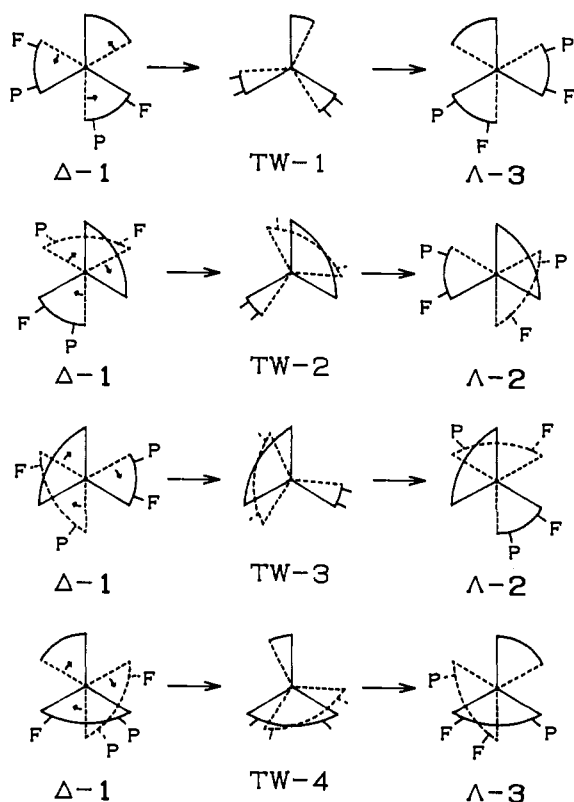


Figure 3. Twist mechanism around the pseudo- C_3 axis (TW-1) and imaginary C_3 axes (TW-2-4). Capital letters F and P designate the substituents trifluoromethyl and phenyl, respectively.

of the facial-meridional isomerization reactions of tris(trifluoromethyl-substituted β -diketonato)ruthenium(III) complexes in DMF.¹⁷ It seems that the activated complexes in such isomerization reactions of (β -diketonato)ruthenium(III) species take relatively restricted or ordered forms.

Probable mechanisms of the isomerization reactions in the present system can be inferred from the observation that the direct conversion between 1 and 3 is forbidden.

Twist mechanisms are considered first. The twist motions about the pseudo- C_3 axis and the three imaginary C_3 axes¹⁸ of $\Delta-1$ are illustrated in Figure 3. The rotation around the pseudo- C_3 axis (via the TW-1 intermediate) or that around one of the three imaginary C_3 axes (via the TW-4 intermediate) brings about the direct conversion between 1 and 3. The present complex has two bulky phenyl groups. According to Fay and Lindmark,¹⁹ the presence of bulky groups can result in unfavorable steric interaction between the groups in the transition state. In light of this steric effect, the rotation via the TW-1 intermediate appears to be the easiest among the four rotations because this intermediate is the only one that has no steric interaction. It is, then, hardly conceivable that this path is forbidden while the paths through TW-2 and TW-3, which are apparently less favorable, are allowed. Consequently, we can exclude the twist mechanisms categorically.

Kinetic studies of similar systems offer several pieces of information that point to bond-rupture mechanisms, as mentioned earlier.¹⁷ Intramolecular rearrangements of tris(β -diketonato)ruthenium(III) complexes in some polar solvents^{9,17} were observed only when the ligands were fluorine-substituted in the systems so far reported, except the case of the tris[(+)-3-acetylcamphorato]ruthenium(III) complex;¹⁰ occurrence of isomerization for the tris(1,1,1-trifluoro-2,4-pentanedionato)ruthenium(III) complex depended on solvents,¹⁷ and the rate constants of the facial-meridional conversion in DMF of a series of tris(trifluoromethyl-substituted β -diketonato)ruthenium(III) complexes were linearly related to the atomic bond population of the Ru-O

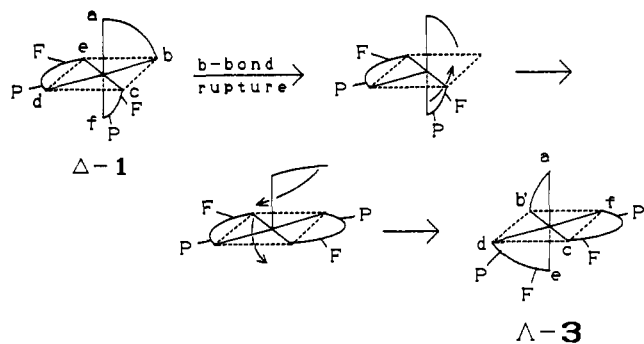


Figure 4. Bond-rupture mechanism via the square-pyramidal intermediate produced by the primary process. Small letters designate the six Ru-O bonds, and capital letters the substituents as shown by Figure 3.

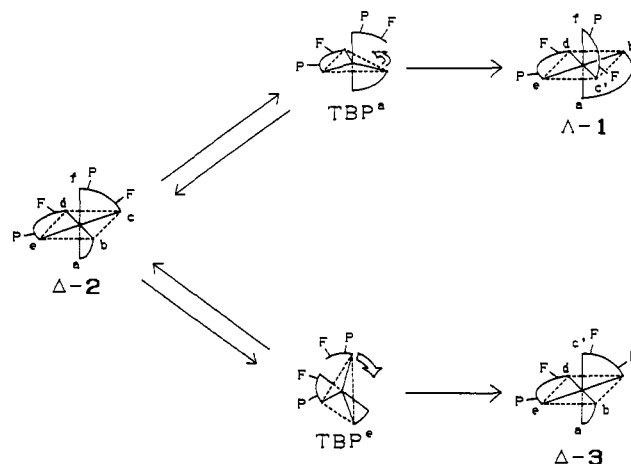


Figure 5. Bond-rupture mechanism via two types of trigonal-bipyramidal intermediates (TBP^a and TBP^e). Small letters designate the Ru-O bonds, and capital letters the substituents.

bonds.¹⁷ Bond-rupture mechanisms deserve close examination.

Generally, two types of intermediates are considered in the bond-rupture mechanisms: square-pyramidal intermediates (SP) and trigonal-bipyramidal intermediates (TBP). Mechanisms are classified according to the geometry of the intermediate and the number of steps involved. Among them, the single rearrangement through a SP intermediate (SP-basal transition state) and the single rearrangement through a TBP intermediate with an axial dangling ligand are indistinguishable, because both intermediates are topologically the same.⁴ The topological correlation diagram for the interconversion of the isomers of the $[M(A-B)_2(C-C)]$ -type complex¹² shows that direct interconversion between $\Delta(\Lambda)-1$ and $\Lambda(\Delta)-3$ is possible through every double rearrangement involving the SP-axial transition state formed by the primary process (SP^p); an example is illustrated in Figure 4. In the case of the double rearrangement through the SP-axial intermediates formed by the secondary process (SP^s), on the other hand, the direct interconversion between 1 and 3 is forbidden for certain bond ruptures and allowed for others. The possible resultant isomers of the SP^p and SP^s pathways are summarized in Table IV for each ruptured bond (the bond designations are given in Figure 1). In order that the SP^s mechanism be compatible with the experiment, we should assume that the reaction proceeds exclusively through the rupture of the *a* or *b* bond of 1 and 3 without any appreciable contribution of SP^p. Such a situation appears quite unlikely, if only because SP^p has priority over SP^s. It is, therefore, more reasonable to exclude the double-rearrangement paths through the SP intermediates.

On the contrary, the single rearrangement through TBP intermediates is compatible with the observation that the direct interconversion between 1 and 3 is forbidden, as seen from the topological correlation diagram.¹² Two distinguishable trigonal-bipyramidal intermediates are formed when a particular bond is ruptured: one with the dangling ligand at an axial position

(18) Springer, C. S., Jr.; Sievers, R. E. *Inorg. Chem.* **1967**, *6*, 852.

(19) Fay, R. C.; Lindmark, A. F. *J. Am. Chem. Soc.* **1983**, *105*, 2118.

Table IV. Ruptured Bond, Intermediate, and Possible Resultant Isomers^a

starting isomer	ruptured bond ^b	intermediate								
		SPP		SP ^a			TBP ^a		TBP ^c	
1	a (M)			3	2	2*		2*	n	
	b (M)			3	2	2*		2*	n	
	c (F)	2	2*	3	2	2*	3*	2*	2	
	d (P)	2	2*	3	1*	2	2*	3	1*	2
	e (F)	2	2*	3	2	2*	3*	2*	2	
	f (P)	2	2*	3	1*	2	2*	3	1*	2
2	a (M)		2*				3*		3*	n
	b (M)		2*		1*		3	1*		n
	c (F)	1*	2*	3	1*	2*	3	1*		3
	d (F)	1	2*	3*	1*	2*	3		2*	1
	e (P)	1	2*	3*	1	2*	3		3*	1
	f (P)	1*	2*	3	1	2*	3		2*	
3	a (M)	1*			2	2*		2*		n
	b (M)	1*			2	2*		2*		n
	c (P)	1*	2	2*	2	2*		2*		2
	d (F)	1*	2	2*	1*	2	2*	3*	3*	2
	e (P)	1*	2	2*	1*	2	2*		2*	2
	f (F)	1*	2	2*	1	2	2*	3*	3*	2

^aKey: n, no net isomerization; asterisk, chirality inverted. ^bThe bond designation is given in Figure 1; symbols M, F, and P (for methyl, tri-fluoromethyl, and phenyl, respectively) denote the substituent nearest the ruptured bond.

(TBP^a) and the other at an equatorial position (TBP^c), as illustrated in Figure 5. The results of the pathways through TBP^a and TBP^c are listed in Table IV. None of these pathways converts 1 to 3 or 3 to 1.

In the single-rearrangement mechanisms through the TBP intermediates, only two types of transition states are available and the degree of ligand motion is more restricted than in the other mechanisms. They thus offer a possible interpretation of the highly negative values of the observed entropy of activation as well. The following discussions, therefore, will be made on the premise that the reaction takes place through TBP^a and/or TBP^c mechanisms (the present study provides no information for distinguishing between the two types of intermediates).

Each observed rate constant, k_{ij} , can be expressed by a linear combination of the rate constants of particular paths if only one bond ruptures at one time according to the first-order rate law:

$$k_{12} = (k_{1F}^c + k_{1F}^e + k_{1M}^a + k_{1M}^b) + (k_{1F}^c + k_{1F}^e + k_{1P}^d + k_{1P}^f) \quad (1)$$

$$k_{21} = (k_{2F}^c + k_{2M}^b) + (k_{2F}^d + k_{2P}^e) \quad (2)$$

$$k_{23} = (k_{2P}^e + k_{2M}^a) + (k_{2F}^c + k_{2P}^f) \quad (3)$$

$$k_{32} = (k_{3P}^c + k_{3P}^e + k_{3M}^a + k_{3M}^b) + (k_{3F}^d + k_{3P}^c + k_{3P}^e + k_{3F}^f) \quad (4)$$

Here k_{iQ}^m ($m = a, b, c, d, e, f; i = 1, 2, 3; Q = M, P, F$) is the rate constant for the path where a particular Ru–O bond m with the nearest substituent Q of isomer i ruptures to form isomer j (j is specified by the second numerical subscript to k). The right-hand-side terms in the first parentheses correspond to TBP^a, and those in the second, to TBP^c.

As the first approximation, we may assume that the rate constant of a particular path is determined solely by the kind of substituent nearest to the ruptured bond regardless of the kind

and geometry of the remaining ligands. This assumption implies that the rate constant for the rupture of a bond nearest to a particular kind of substituent is the same in any isomer. Then, eqs 1–4 reduce to

$$k_{12} = (2k_F + 2k_M) + (2k_F + 2k_P) \quad (5)$$

$$k_{21} = (k_F + k_M) + (k_F + k_P) \quad (6)$$

$$k_{23} = (k_P + k_M) + (k_F + k_P) \quad (7)$$

$$k_{32} = (2k_P + 2k_M) + (2k_P + 2k_F) \quad (8)$$

or $k_{12}/k_{21} = 2.0$ and $k_{23}/k_{32} = 0.5$. These values are not very different from the observed values of K_{12} and K_{23} (Table I), but the discrepancies are beyond the experimental errors. The above assumption, therefore, is not strictly valid. In other words, the rate of rupture of an Ru–O bond is influenced not only by the nearest substituent but also by other environments inside and outside the molecule. The observed values of K_{12} (≈ 1.8) and K_{23} (≈ 0.7) suggest that the rates of bond rupture in 2 are generally larger than the rates of rupture of the corresponding bonds in the other isomers. With eqs 2 and 3, the experimental values of k_{21}/k_{23} , which are larger than unity (Table II), lead to the following relations:

$$k_{2F}^c + k_{2M}^b > k_{2P}^e + k_{2M}^a \quad (\text{TBP}^a)$$

$$k_{2F}^d + k_{2P}^e > k_{2F}^c + k_{2P}^f \quad (\text{TBP}^c)$$

$$k_{2F}^d + k_{2M}^b > k_{2P}^e + k_{2M}^a \quad (\text{TBP}^a + \text{TBP}^c)$$

The interpretation of these inequalities seems difficult at the present stage.

Acknowledgment. We are grateful to Dr. Y. Satsu, Hitachi Seisakusho Co. Ltd., for his helpful discussion. Thanks are also due Dr. S. F. Howell, Sophia University, for correcting the manuscript.